R. Bras. Zootec., 55:e20250061, 2026
https://doi.org/10.37496/rbz5520250061

Breeding and genetics
Full-length research article

Revista Brasileira de Zootecnia

Brazilian Journal of Animal Science
e-ISSN 1806-9290
www.rbz.org.br

Transcriptome and microbiome reveal key genes and colonic microorganisms affecting fat deposition in Tunchang pigs

Guiqing **Huang**[1,2], Yunchao **Zhang**[1,2], Jiayi **He**[1,2], Chen **Peng**[1,2], Kaiyu **Chen**[1,2], Zhengguang **Wang**[1,2*]

[1] Zhejiang University, Hainan Institute, Sanya, China.
[2] Zhejiang University, College of Animal Science, Hangzhou, China.

***Corresponding author:**
wzhguang68@zju.edu.cn

Received: May 1, 2025
Accepted: February 2, 2026

How to cite: Huang, G.; Zhang, Y.; He, J.; Peng, C.; Chen, K. and Wang, Z. 2026. Transcriptome and microbiome reveal key genes and colonic microorganisms affecting fat deposition in Tunchang pigs. Revista Brasileira de Zootecnia 55:e20250061.
https://doi.org/10.37496/rbz5520250061

Editors:
Lucas Lima Verardo
Ana Fabrícia Braga Magalhães

Copyright: This is an open access article distributed under the terms of the Creative Commons Attribution License (http://creativecommons.org/licenses/by/4.0/), which permits unrestricted use, distribution, and reproduction in any medium, provided the original work is properly cited.

ABSTRACT - To investigate the key genes and microorganisms that influence fat deposition in Tunchang (TC) pigs, fourteen clinically healthy 320-day-old TC sows (body weight: 86.00 ± 2.30 kg) were stratified into high-backfat (HBF, n = 7) and low-backfat (LBF, n = 7) groups according to the difference in backfat thickness. RNA sequencing was employed to analyze hepatic transcriptomes, with subsequent identification of differentially expressed genes (DEGs) and their biological functions. In parallel, 16S rRNA sequencing and short-chain fatty acid (SCFA) quantification were conducted to characterize microbial community structure and metabolic profiles in intestinal contents across adiposity phenotypes. Transcriptomic profiling identified key regulators including *PLIN2*, *CEL*, *CYP7A1*, *AMY2* and *SLC34A2* associated with fat deposition, while microbiome analysis revealed significant correlations between *Desulfovibrio*, *Succinivibrio*, *Faecalibacterium*, and *Treponema* genera with SCFA dynamics. Low-backfat pigs may synergistically reduce fat deposition through enhanced fatty acid degradation at both the host gene and microbial levels. The findings elucidate potential mechanisms governing fat deposition in indigenous pig breeds, which not only provides candidate genes for molecular marker assisted breeding of local pigs and offering new insights into improving fat deposition through microbial regulation.

Keywords: backfat thickness, differentially expressed gene, microbe, sequencing

1. Introduction

Chinese indigenous pig breeds exhibit greater fat deposition capacity (Poklukar et al., 2020), which is evidenced in meat quality by higher intramuscular fat content and improved fatty acid composition (Chen et al., 2022). However, excessive fat deposition not only induces obesity but also adversely affects growth rates and reproductive performance (Houde et al., 2010; Hausman et al., 2014; Thiengpimol et al., 2022). Consequently, elucidating the mechanisms underlying fat deposition traits in indigenous pigs is important for improving production efficiency.

RNA sequencing has been widely used in recent years to facilitate the systematic dissection of gene regulatory networks associated with fat deposition. A recent study in Ningxiang pigs identified differentially expressed genes that were significantly enriched in lipid binding, fatty acid β-oxidation, and glycerol-lipid metabolism pathways, highlighting specific regulatory mechanisms (Wang et al., 2023b).

Further evidence demonstrated that lipogenic genes were more highly expressed in adipose tissue of obese pigs compared withlean pigs, while the lipolysis marker *perilipin2* (*PLIN2*) mRNA levels were markedly reduced (Qiu et al., 2017). The liver, as a central metabolic organ (Lyu et al., 2022), orchestrates systemic lipid homeostasis through fatty acid synthesis, β-oxidation, and lipoprotein transport (Albuquerque et al., 2020; Zhang et al., 2022). However, current research on porcine fat deposition predominantly focuses on adipose tissue (Xing et al., 2019) and muscle (Li et al., 2023) leaving the hepatic transcriptional mechanisms underlying fat deposition in indigenous breeds largely unexplored.

Notably, fat deposition is a complex trait influenced not only by host genetics but also by the gut microbiome. The critical role of gut microbiota in regulating energy harvest, lipid metabolism, and fat storage has been increasingly recognized (Yang et al., 2018; Schoeler and Caesar, 2019). For instance, obese pigs usually exhibit higher gut microbial diversity and greater fatty acid production compared with lean pigs (Xiao et al., 2018). Short-chain fatty acids (SCFA), which are metabolites produced by the gut microbiota, also play important roles in adipogenesis regulation. For example, butyric acid inhibits adipogenesis through the activation of the G protein-coupled receptor and inhibition of fatty acid synthase expression, whereas acetic acid promotes preadipocyte differentiation through the regulation of histone deacetylases (Fusco et al., 2023). Furthermore, recent studies have further demonstrated that microbial functional genes regulate fat deposition through metabolites (Ma et al., 2024).

Despite the independent advancements in both hepatic transcriptomics and gut microbiome research, our understanding of their interactive effects on fat deposition remains limited. Therefore, integrative transcriptomic and microbiome analyses are needed to unravel the complex network of host genes and colonic microorganisms involved in the co-regulation of fat deposition in pigs.

Tunchang (TC) pigs, indigenous to Hainan Province, China, are recognized for their superior meat quality and adaptability to coarse feed (Liu et al., 2024). Nevertheless, their high backfat thickness and low lean meat percentage limit their commercial value. Previous studies have characterized the genetic structure (Wang et al., 2023a; Zhong et al., 2023) and gut microbiota profiles (He et al., 2023; Tan et al., 2024) of TC pigs; however, studies focusing on fat deposition traits in this breed remain scarce.

This study aimed to reveal key genes and colonic microorganisms affecting fat deposition in TC pigs by elucidating transcriptome and microbiota data. These findings may contribute to improving animal performance and production efficiency in indigenous pig breeds.

2. Material and methods

2.1. Animals and sample collection

The study was designed and implemented followed the protocol number of GBT 35892-2018, and it was reviewed and approved by Animal Care and Use Committee.

A total of 14 healthy 320-day-old TC sows (body weight: 86.00 ± 2.30 kg) were provided by a local commercial farm (Tunchang, China). After slaughter, backfat thickness was meticulously measured using a vernier caliper (GuangLu brand) according to the national standard (NY/T 825-2004). The average value from three key anatomical locations (shoulder, last rib, and thoracolumbar junction) was calculated for each individual. Based on these average values, animals were stratified into two distinct groups: the top seven individuals were assigned to the high backfat thickness (HBF, n = 7) group, with an average backfat thickness of 50.97 ± 2.53 mm, while the bottom seven formed the low backfat thickness (LBF, n = 7) group, with an average backfat thickness of 39.48 ± 0.42 mm. The difference in backfat thickness between groups was highly significant ($P<0.001$). Fresh liver tissue was rapidly collected and frozen in liquid nitrogen immediately, and stored at −80 °C until RNA extraction.

2.2. Transcriptome sequencing of liver tissue

2.2.1. RNA extraction, library preparation and sequencing

Prior to RNA extraction, frozen liver samples were thoroughly ground into a fine powder in liquid nitrogen using a pre-cooled mortar and pestle to prevent RNA degradation. A precisely weighed amount of the powdered tissue, measured using a high-precision electronic balance (Adam brand), was immediately transferred to a tube containing lysis buffer for subsequent homogenization and RNA extraction. Total RNA was then isolated from liver tissue using the Total RNA Kit II (OMEGA, Norcross, GA, USA) according to the manufacturer's instructions. RNA quality and integrity were assessed using a NanoDrop spectrophotometer (Thermo Scientific). All samples used for library construction exhibited 28S/18S rRNA ratios ranging from 1.8 to 2.2 and RNA concentrations between 350 and 550 ng/μL, confirming the high integrity and purity of the extracted RNA.

Sequencing libraries were generated according to the following steps: mRNA was purified from total RNA using poly-T oligo-attached magnetic beads. Fragmentation was carried out using divalent cations under elevated temperature in an Illumina proprietary fragmentation buffer. First strand cDNA was synthesized using random oligonucleotides and Super Script II. Second strand cDNA synthesis was subsequently performed using DNA Polymerase I and RNase H. Remaining overhangs were converted into blunt ends via exonuclease/polymerase activities and the enzymes were removed. After adenylation of the 3' ends of the DNA fragments, Illumina PE adapter oligonucleotides were ligated to prepare for hybridization. To select cDNA fragments of the preferred 400-500 bp in length, the library fragments were purified using the AMPure XP system (Beckman Coulter,Beverly, CA, USA). DNA fragments with ligated adaptor molecules on both ends were selectively enriched using Illumina PCR Primer Cocktail in a 15 cycle PCR reaction. Products were purified (AMPure XP system) and quantified using the Agilent high sensitivity DNA assay on a Bioanalyzer 2100 system (Agilent). The sequencing library was then sequenced on NovaSeq 6000 platform (Illumina).

2.2.2. Data quality control and sequence alignment

The raw sequencing data (FASTQ format) were processed using Cutadapt (v3.4) to remove adapter sequences and low-quality reads and generated in this study have been deposited in the National Genomics Data Center (NGDC), part of the China National Center for Bioinformation (CNCB), under BioProject accession number PRJCA045892 (https://ngdc.cncb.ac.cn/bioproject/browse/PRJCA045892). Clean reads were aligned to the Sus scrofa reference genome (GCF_000003025.6), which was published on Feb 7, 2017. The alignment was performed using HISAT2 (v2.2.1) with ≤1 mismatch tolerance. For gene annotation, the corresponding annotation file was obtained from the same source and version as the reference used. Gene expression levels were normalized as FPKM (Fragments Per Kilobase per Million mapped reads), and genes with FPKM >1 were retained for downstream analysis.

2.2.3. Identification and functional enrichment of DEGs

DEGs were identified using DESeq2 (v1.34.0) in R (v4.2.1) with thresholds of |log2FoldChange| >1 and P-value <0.05. Gene Ontology (GO) enrichment analysis and Kyoto Encyclopedia of Genes and Genomes (KEGG) pathway analysis were performed using the R packages "topGO" (v2.48.0) and "cluster Profiler" (v4.4.4), respectively. Statistical significance was assessed by P-value <0.05.

2.2.4. Protein-protein interaction (PPI) network analysis

Differentially expressed genes (DEGs) were queried in the STRING database (v11.5) to predict protein interactions. To ensure high-confidence interactions and control for false positives, a minimum confidence (combined) score threshold of > 0.7 was applied, which is a stringent criterion widely adopted in the field. The STRING database itself integrates evidence from multiple sources and

calculates this confidence score, which accounts for the non-independence of evidence and effectively serves as a robust statistical control. The resulting PPI network was visualized and analyzed using Cytoscape (v3.9.1). Key functional modules were identified through Molecular Complex Detection (MCODE) clustering.

2.3. 16S rRNA sequencing of colon contents

2.3.1. ample collection and DNA extraction

Fresh colon contents (200 mg) were collected under aseptic conditions and immediately stored at −80 °C. Prior to DNA extraction, these contents were thoroughly ground following the same procedure previously described for liver tissues. Total microbial genomic DNA was extracted using the instructions of the DNA extraction kit (QIAGEN, Duesseldorf, Germany). Total microbial genomic DNA was extracted according to the instructions of the DNA extraction kit (QIAGEN, Duesseldorf, Germany), and the concentration and purity of DNA were determined by 1% agarose gel electrophoresis (Invitrogen, Carlsbad, CA, USA) using a NanoDropND-1000 spectrophotometer (Thermo Fisher Scientific, Waltham, MA, USA) to determine the total amount of DNA.

2.3.2. PCR amplification and library preparation

The PCR reaction system (25 μL) was configured as follows: 5×reaction buffer 5 μL, 5×GC buffer 5 μL, dNTP (2.5 mM) 2 μL, upstream primer (10 μM) 1 μL, downstream primer (10 μM) 1 μL, DNA template 2 μL, ddH_2O 8.75 μL, Q5 DNA polymerase 0.25 μL. The amplification parameters were set as follows: pre-denaturation at 98 °C for 2 min, denaturation at 98 °C for 15 s, annealing at 55 °C for 30 s, extension at 72 °C for 30 s, 30 cycles, and extension at 72 °C for another 5 minutes. The PCR amplified products were detected by 2% agarose gel electrophoresis, and the target fragments of about 500 bp size were cut and recovered using the Gel Recovery Kit. Sequencing libraries were prepared using the TruSeq Nano DNA LT Library Prep Kit (Illumina, San Diego, CA, USA), and paired-end sequencing was performed using MiSeq PE250 sequencer.

2.3.3. 16S data processing and analysis

Raw sequences were quality-filtered using Trimmomatic (v0.39), and primer sequences were removed using Cutadapt (v3.5). Amplicon sequence variants were generated through DADA2 denoising in QIIME2 (v2022.2). Taxonomic classification was performed using a pretrained naïve Bayesian classifier (confidence threshold: 0.7) based on the Greengenes database (v13_8_99). Alpha diversity indices, including Chao1, observed species, Shannon, and Simpson indices, and beta diversity based on Bray-Curtis principal coordinate analysis (PCoA) were calculated using the vegan v2.6-4 package in R (v4.2.2). Linear discriminant analysis effect size (LEfSe) was applied to identify microbial biomarkers, using an LDA score threshold of >2.0.

2.3.4. Determination of SCFA in colon contents

The concentration of SCFA in colonic contents was determined by gas-liquid spectrometry-mass spectrometry (Han et al., 2018). Briefly, approximately 100 mg of sample was accurately weighed using a high-precision electronic balance (Adam brand) and homogenized in 500 μL of sterile water with glass beads via a high-throughput tissue homogenizer. After centrifugation at 12,000 rpm for 10 min at 4 °C, 200 μL of the supernatant was collected and acidified with 100 μL of 15% phosphoric acid. Subsequently, 20 μL of internal standard solution (4-methylvaleric acid, 375 μg/mL in ether) and 280 μL of ether were added for liquid-liquid extraction. The mixture was vortexed vigorously for 1 min and centrifuged again under the same conditions. The upper ether phase was then transferred to a GC vial for analysis using a Thermo TRACE 1300 gas chromatograph coupled with a Thermo ISQ

7000 mass spectrometer (Thermo Fisher Scientific, USA). Each sample was prepared in triplicate, and the relative standard deviation (RSD) was maintained below 15%. The final SCFA concentrations are reported in μg/mL.

2.4. Statistical analysis

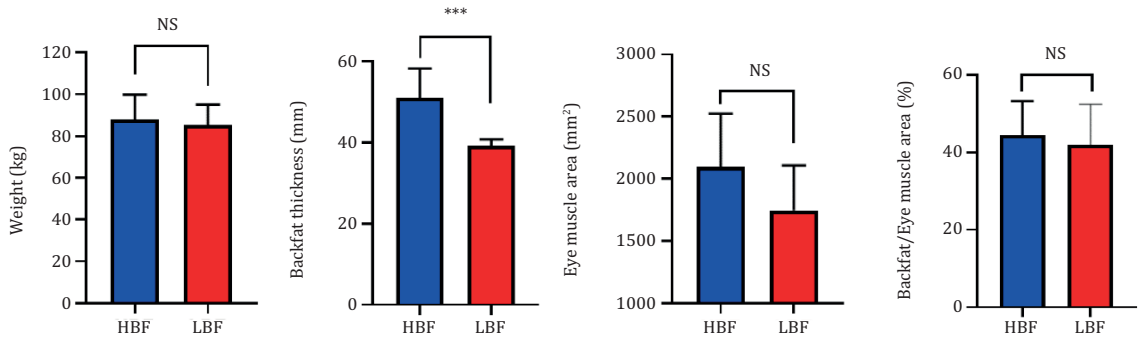
All data were expressed as the mean ± SEM, the differences between the HBF and LBF groups were analyzed using either the standard unpaired Student's t-test (for data with homogeneous variances) or the unpaired t-test with Welch's correction (for data with heterogeneous variances). For subsequent pairwise comparisons, the Benjamini-Hochberg false discovery rate (FDR) procedure was applied to correct the P-values for multiple testing. Differences were considered statistically significant at FDR-adjusted P-values <0.05.

Spearman correlation analysis was conducted to explore the linear relationships between the relative abundance of colonic microbiota and SCFA levels. Prior to analysis, microbial abundance data were log-transformed to reduce skewness. The correlation was calculated by a R package vegan (version 2.7-2). This analysis generated a correlation matrix. Results were visualized as a R package pheatmap (version 1.0.13).

3. Results

3.1. Differences in phenotypic traits

An extremely significant disparity in backfat thickness was confirmed between the HBF and LBF TC pigs (HBF: 50.97 ± 2.74 mm vs. LBF: 39.22 ± 0.21 mm (P<0.001; Figure 1). Although the LBF group showed a trend toward lower body weight compared with the HBF group, this difference did not reach statistical significance (P>0.05). No significant differences were observed in the ratio of backfat thickness to eye muscle area between the two groups.

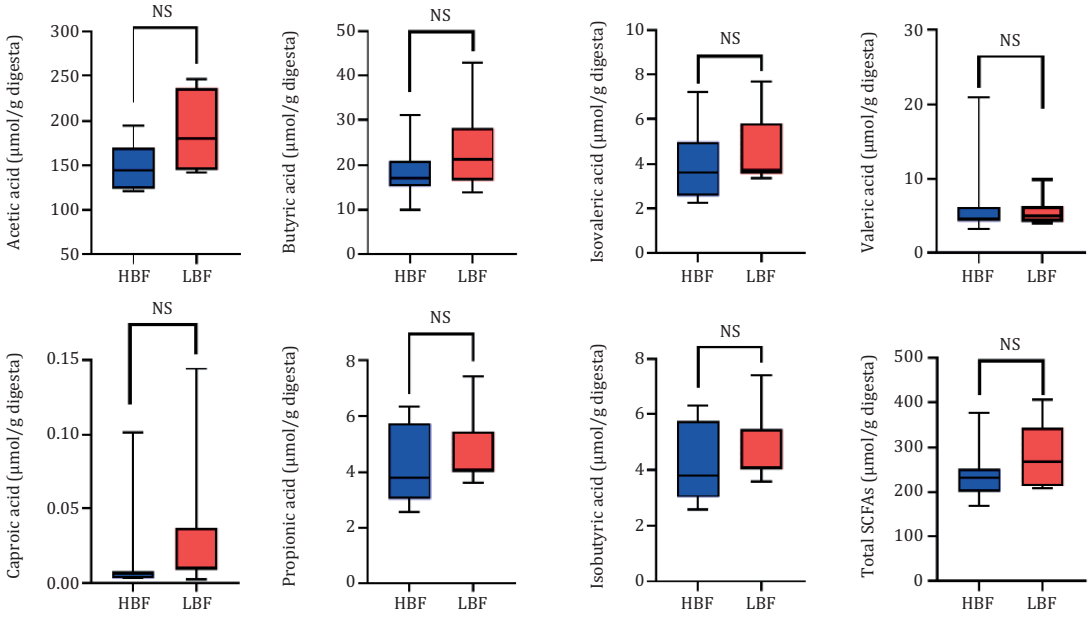


HBF - high backfat thickness; LBF - low backfat thickness.

Figure 1 - Measurements of body weight, backfat thickness, and eye muscle area of Tunchang pigs.

3.2. Differences in SCFA concentration

The concentration of total SCFA in the colonic contents of TC pigs did not change significantly (P>0.05; Figure 2) in the HBF and LBF groups, but the concentration was higher in the LBF group than in the HBF. Acetic acid had the highest concentration, followed by butyric acid, and caproic acid had the lowest concentration, which were all higher in the LBF group than in the HBF group.



HBF - high backfat thickness; LBF - low backfat thickness.

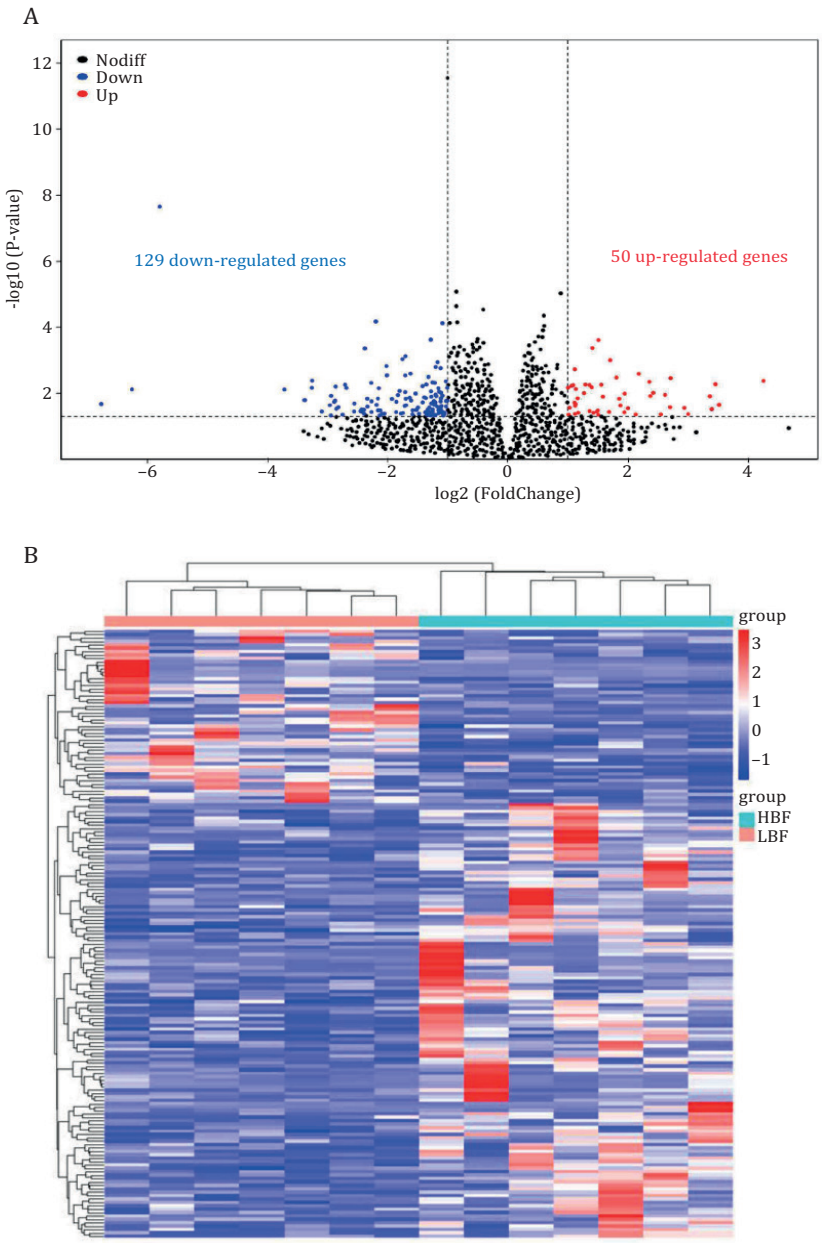
Figure 2 - The short-chain fatty acid (SCFA) concentration in the colon in Tunchang pigs. SCFA include acetic acid, butyric acid, isovaleric acid, valeric acid, caproic acid, propionic acid, isobutyric acid and total SCFA.

3.3. Evaluation of sequencing data

In accordance with the Illumina Data Quality Assessment Guidelines, the sequence quality score Q30 for each sample was higher than 90.40%. The clean data of each sample was aligned to the reference genome (Sus scrofa 11.1), with a matching success rate of 95%, and on average, approximately 75% of the reads were mapped to exons, 5.8% to introns, and 3.7% to intergenic regions. The data above suggest that the sequencing data quality is extremely high and appropriate for further analysis.

3.4. Transcriptome differences between HBF and LBF groups

According to the thresholds of |log2FoldChange|>1 and P-value <0.05, 179 DEGs were identified between the HBF and LBF groups, of which 50 genes were up-regulated and 129 genes were down-regulated in the LBF group (Figure 3A). Cluster analysis based on the expression levels of DEG in different samples and the expression patterns of different genes in the same sample revealed that there were large differences in the expression patterns of DEG in different groups (Figure 3B). Based on the differential expression analysis, we identified a set of genes with established roles in lipid metabolism and fat deposition. These key candidates included *Solute Carrier Family 34 Member 2* (*SLC34A2*), *ATP Binding Cassette Subfamily C Member 11* (*ABCC11*), *Perilipin 2* (*PLIN2*), *Carboxyl Ester Lipase* (*CEL*), *Cytochrome P450 Family 11 Subfamily A Member 1* (*CYP11A1*), *Cytochrome P450 Family 7 Subfamily A Member 1* (*CYP7A1*) and *Amylase Alpha 2B* (*AMY2*) etc.



A - Volcano plot. The red colour indicates an increase in gene expression, while the blue colour indicates a decrease. B - Cluster diagram of DEG. The horizontal axis represents the individual number, while the vertical axis depicts DEG. DEG - differentially expressed gene.

Figure 3 - Statistical results of DEG.

3.5. Functional enrichment analysis of DEGs

The top 20 significantly enriched GO terms were most abundant in the molecular function section, such as alpha-amylase activity, protein binding involved in heterotypic cell-cell adhesion, phosphatidylserine binding, and so on, which are related to material metabolism and energy metabolism (Figure S1). In terms of biological processes, they are mainly enriched in cell proliferation, adhesion, and neuromodulation; in terms of cellular components, they are mainly enriched in cell structure and immunity. The top 20 significantly enriched KEGG pathways were found and several of the significantly enriched pathways may be related to fat deposition: Peroxisome proliferator-activated

receptor (PPAR) signaling pathway, phosphatidylinositol 3-kinase/protein kinase (PI3K-Akt) signaling pathway, calcium signalling pathway and others (Figure S2).

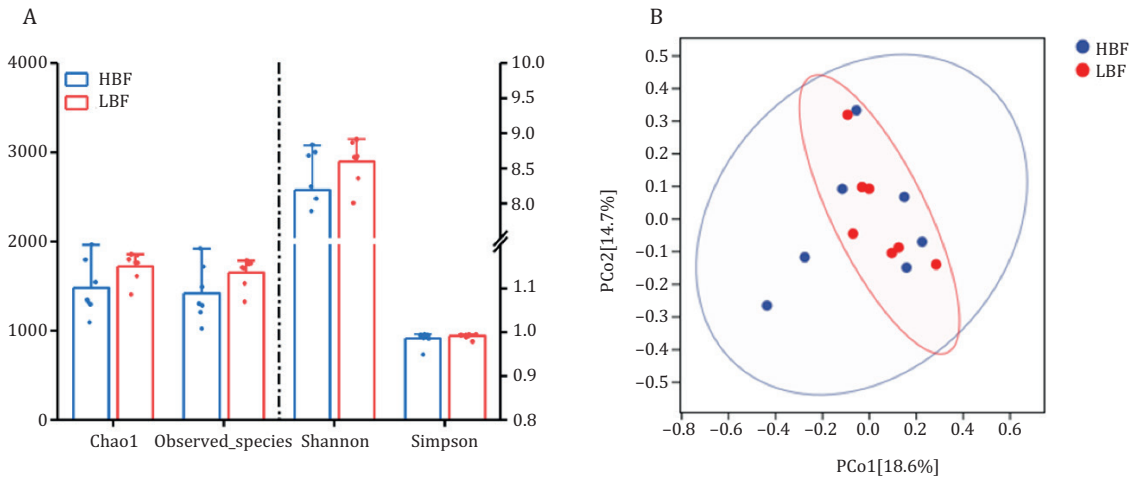
3.6. PPI network analysis

The mutual regulation and functional relationship of DEG were subjected to further exploration via a PPI analysis (Figure S3). Genes such as *AMY2*, *SLC34A2*, and *PLIN2* had a high number of connected nodes in the graph, predicting that they may play important roles in lipid metabolism. Among them, *AMY2* is a starch digesting enzyme, and the energy generated from the digestion process can be converted into the form of triglycerides to be stored in adipose tissue; the *SLC34A2* gene encodes a calcium salt transport protein, and calcium plays an important role in cell signalling, adipocyte differentiation, and lipid metabolism; therefore, changes in the expression of *SLC34A2* may affect fat deposition.

3.7. Composition of colon flora

An as-yet-unidentified mechanism regulating lipid metabolism may exist between the host and gut microbiota. Alpha diversity analysis showed that none of the evaluated indices differed significantly (P>0.05) between the HBF and LBF groups (Figure 4A). However, the gut microbial community of the LBF group exhibited higher species richness (Chao1 and Observed_species indices) and greater Shannon diversity. Based on the Bray-Curtis distance matrix, principal coordinate analysis (PCoA) was performed to evaluate the colonic microbial communities of TC pigs. PCoA1 and PCoA2 explained 18.6% and 14.7% of the total variance, respectively (Figure 4B). Samples from the HBF and LBF groups showed a trend toward partial segregation along PCoA1 and PCoA2, suggesting slight differences in microbial community structure between groups. These differences may be associated with specific bacterial taxa rather than with overall microbial diversity changes.

At the phylum level, Bacteroidetes and Firmicutes were the most abundant phyla, accounting for more than 85% of the microbial community (Figure 5A), with no significant differences observed between groups (P>0.05). In addition, the abundance of Proteobacteria was significantly higher in the HBF

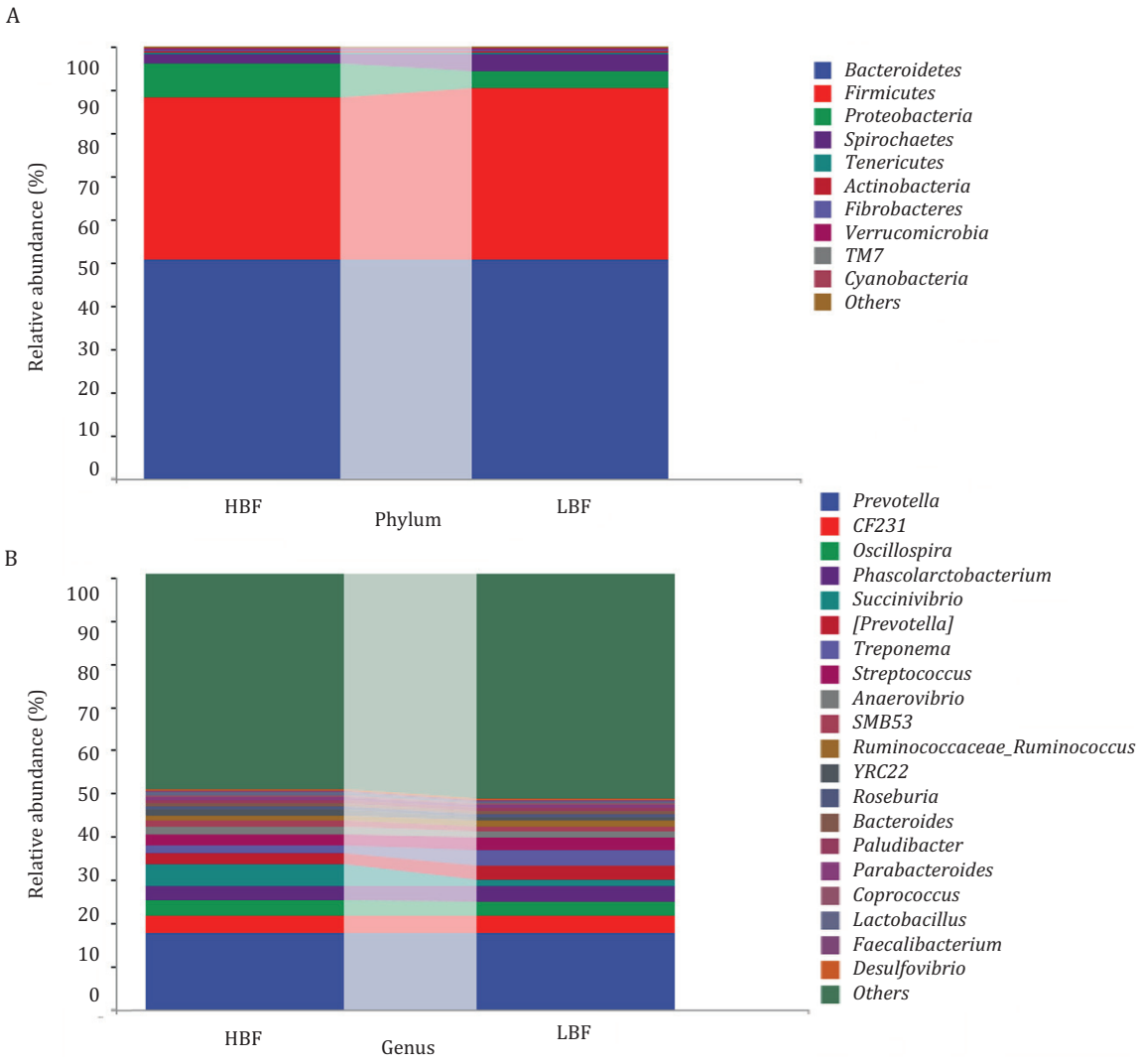


A - α-diversity of the colon microbiome. The Chao1, observed species, Shannon, and Simpson indices were used for evaluation. B - Principal coordinate analysis of the colon microbiome. Each point in the figure represents a sample, with different colored points indicating different groups.

Figure 4 - Microbial diversity analysis of the colon in Tunchang pigs.

group than in the LBF group, whereas the abundance of Spirochaetes was nearly doubled in the LBF group, suggesting that the intestinal tract of pigs with low backfat thickness may be more conducive to the colonization of fiber-degrading bacteria.

At the genus level (Figure 5B), the top eight genera in relative abundance were *Prevotella*, *CF231*, *Oscllospira*, *Phascolarctobacterium*, *[Prevotella]*, *Succinivibrio*, *Streptococcus*, and *Treponema*. The abundance of *Succinivibrio*, *Desulfovibrio*, *Lactobacillus*, and *YRC22* in the LBF group was lower than that of the HBF group, respectively, whereas the abundance of *Faecalibacterium* and *Treponema* was higher than that of the HBF group. Among them, the difference in the abundance of *Desulfovibrio* was statistically significant ($P<0.05$). As shown in the Figure S4, g__*Desulfovibrio*, *g__Dorea*, *o__Hydrogenophilales*, *f__Hydrogenophilaceae*, *g__Thiobacillus*, *f__Dethiosulfovibrionaceae*, *p__Synergistetes*, *c__Synergistia*, *o__Synergistales*, the relative abundance of gut microorganisms was significantly increased in HBF, and f__*RF16* and *o__RF32* microorganisms were significantly increased in LBF.



A - phylum level; B - genus level.

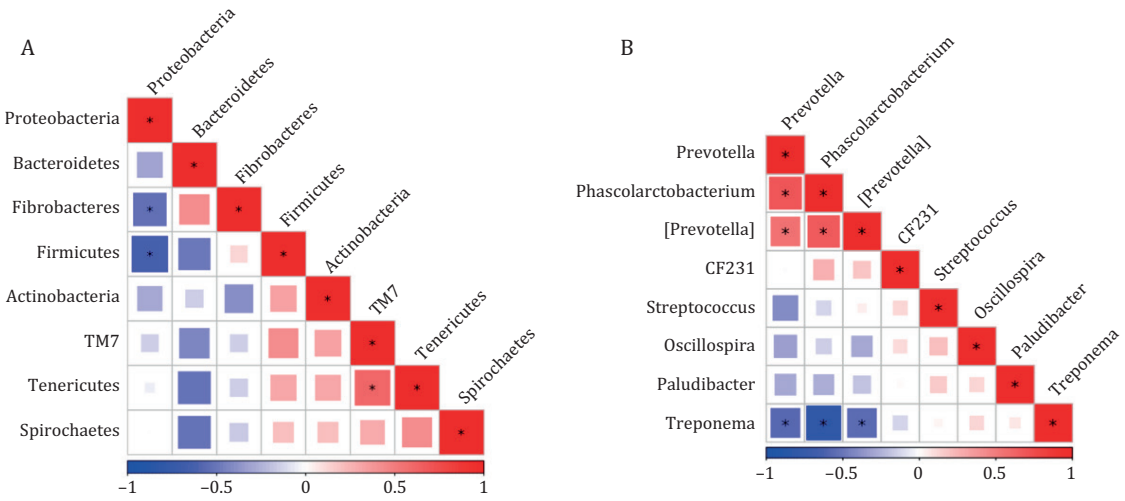
Figure 5 - Composition of major microbial communities and their relative abundance at different taxonomic levels in the colons of Tunchang pigs.

3.8. Correlation analysis between colonic cicrobiota

To assess potential interactions in the colonic microbiome of TC pigs, Spearman correlation analysis was carried out across phylum and genus taxa. Our analysis identified several significant correlations (Figure S5). At the phylum level, Proteobacteria showed significant negative correlations with *Fibrobacteres* and Firmicutes, while *Tenericutes* was positively correlated with TM7 (P<0.05). No significant correlations were detected between Bacteroidetes and *Tenericutes* or *Spirochaetes*. Among genera, a significant positive correlation network linked *Prevotella*, *Phascolarctobacterium*, and [*Prevotella*]. The *Treponema*, however, was found to be significantly negatively correlated with both *Prevotella* and *Phascolarctobacterium* (P<0.05).

3.9. Correlation analysis of colonic cicroorganisms with SCFA

Correlation analysis of the content of SCFA was performed by Spearman's correlation coefficient and Mantel's test for the top 20 genera and SCFA in the colon of TC pigs in the LBF group. As shown in Figure 6, the genera that showed significant positive correlation with acetic acid were *Prevotella* (r = 0.533, P = 0.004), *Bacteroides* (r = 0.355, P = 0.022), *Parabacteroides* (r = 0.353, P = 0.048, and *Phascolarctobacterium* (r = 0.310, P = 0.031), suggesting that they may promote dietary fiber catabolism and thus acetic acid synthesis. In addition, *Treponema* and acetic acid had a low but statistically significant correlation (r = 0.248, P = 0.047). The genera that showed significant positive correlation with butyric acid were *Prevotella* (r = 0.616, P = 0.000) and *Desulfovibrio* (r = 0.574, P = 0.007) suggesting that they play an important role in butyric acid production. Genus associated with propionic acid: *Prevotella* again showed a strong positive correlation (r = 0.472, P = 0.010), suggesting a broad metabolic capacity across multiple classes of SCFA. Genus associated with isovaleric acid: *Prevotella* showed a significant positive correlation in isovaleric acid (r = 0.427, P = 0.009) and also in isobutyric acid (r = 0.352, P = 0.030), suggesting that it may be involved in the degradation of branched-chain amino acids to produce branched-chain SCFA. *Desulfovibrio* was significantly positively correlated in both isovaleric acid (r = 0.422, P = 0.014) and isobutyric acid (r = 0.410, P = 0.027), further supporting its versatile metabolic potential.



A - phylum level; B - genus level. * P<0.05; ** P<0.01.

Figure 6 - Spearman's correlation of colonic microbial in Tunchang pigs.

4. Discussion

In this study, liver tissues from TC pigs with different backfat thicknesses were analyzed by RNA Sequencing, and a total of 179 DEG were identified based on the criteria of |log2FoldChange|>1 and P-value<0.05. DEG were significantly enriched in PPAR signaling pathway and PI3K-AKT signaling pathway, which together suggested that the liver may synergistically regulate lipid deposition by enhancing lipid oxidation and inhibiting lipid synthesis.

Among them, *PLIN2*, *CEL*, *CYP7A1*, *AMY2,* and *SLC34A2* were identified as key regulators of fat deposition by KEGG annotation and PPI analysis. The conventional view is that *PLIN2* promotes lipid storage by stabilizing lipid droplets, but recent studies have shown that it may regulate the rate of lipolysis through interactions with adipose triglyceride lipase (Kersten, 2014). The upregulation of *PLIN2* in this study may avoid oxidative stress induced by excessive lipolysis by regulating the rate of lipolysis. The functional significance of this protective lipolysis pattern in low backfat pig breeds deserves further investigation (Sztalryd and Brasaemle, 2017). Secondly, *CEL* is a key enzyme for dietary cholesterol ester hydrolysis, and its reduced activity in the LBF group can directly inhibit exogenous lipid uptake (Hui and Howles, 2002). Combined with the background that TC pigs have been adapted to tropical low-fat diets for a long period of time, the specific down-regulation of *CEL* may reflect their unique nutritional adaptation strategy. Notably, the significant down-regulation of *AMY2*, a key enzyme of sugar metabolism, in the LBF group indicated the ability to limit the energy utilization of exogenous carbohydrates. This mechanism synergizes with the *CEL* mediated inhibition of exogenous lipid uptake, which jointly shapes the metabolic characteristics of the liver in TC pigs as restricting lipid synthesis and increasing endogenous oxidation, which is distinctly different from that of other pig breeds that rely on adipose tissue for lipid storage, and highlights the pivotal role of the liver in the regulation of backfat thickness in TC pigs.

Differences in backfat thickness are closely related to liver-specific lipid metabolism network in TC pigs. PPAR is involved in adipocyte differentiation and can promote the differentiation of preadipocytes into mature adipocytes, and PI3K-Akt is closely related to PPAR through phosphorylation and regulation of several transcription factors and enzymes to promote glycogen and fatty acid synthesis, favouring lipid storage. These analyses may help to explain the molecular mechanisms underlying the differences in fat deposition in TC pigs. Pan et al. (2022) compared the dorsal adipose tissue of Duroc and Luchuan (DL) pigs and found that DEG were mainly enriched in lipid metabolism, storage, and transport pathways; Deng et al. (2023) found that the DEG identified in the skeletal muscles of DL pigs were enriched in the pathways related to glucose and lipid metabolism, both of which were consistent with the present study. Downregulation of *PLIN2* has been demonstrated to promote lipolysis by reducing the stability of lipid droplet-encapsulated proteins (Tsai et al., 2017), whereas high expression of *CEL* has been shown to accelerate the process of β-oxidation by hydrolyzing triglycerides to release free fatty acids (El Jellas et al., 2022). Notably, upregulation of *CYP7A1* has been shown to drive bile acid synthesis and inhibit fatty acid synthase through activation of the farnesol X receptor (Chambers et al., 2019). This is consistent with the fact that transgenic mice overexpressing *CYP7A1* are able to resist obesity, fatty liver, and diabetes mellitus induced by a high-fat diet (Qi et al., 2015). Furthermore, the analysis revealed that the expression of genes related to the PPARα pathway, including *ATP1A2* and *CYP7A1*, was increased in the LBF group. These findings further support the hypothesis that enhanced hepatic fatty acid catabolism plays a pivotal role in the development of the low-backfat phenotype.

The liver, a central organ of metabolism in the body, has been found to be primarily involved in fatty acid degradation processes (Reiter et al., 2007; Ponziani et al., 2015). In addition, advances in microbiome research have demonstrated that specific bacterial genera also play important roles in shaping the host obesity phenotype (Aron-Wisnewsky et al., 2021; Portincasa et al., 2022). In this study, we assessed the α-diversity, β-diversity, and species composition characteristics of colonic microbial communities in TC pigs with different backfat thicknesses by 16S rRNA sequencing. Correlation analysis revealed that *Prevotella*, *Desulfovibrio*, *Faecalibacterium*, and *Treponema* genera regulate host fat deposition through SCFA-associated metabolic networks.

Fat deposition traits in TC pigs are closely related to the adaptive evolution of their intestinal flora, and the composition of the colonic flora in the LBF and HBF groups showed a significant divergence. the LBF group was more abundant in *Faecalibacterium* and *Treponema* than the HBF group, respectively, while the HBF group was specifically enriched in *Desulfovibrio*, *Lactobacillus* and *Succinivibrio* genera in the HBF group were higher than those in the LBF group, respectively. This difference reflects the adaptive selection of gut flora to the metabolic phenotype of the host, which has been corroborated by studies in other pig breeds. Further analysis revealed higher concentrations of SCFA in the LBF group compared with the HBF group, suggesting a correlation between enhanced SCFA production and the presence of the lean muscle phenotype. This finding aligns with earlier research (Yan et al., 2017), providing further evidence for the potential implications of SCFA production in relation to the lean muscle phenotype.

The LBF group marker flora inhibited fat deposition through the metabolism of SCFA. The high abundance of *Faecalibacterium* and *Treponema* was a distinctive feature of LBF pigs. *Faecalibacterium* as a major producer of butyric acid ($P<0.05$) may activate the PPAR signaling pathway through butyric acid and upregulate fatty acid oxidase expression and promoting mitochondrial β-oxidation (Wen et al., 2021). Reduced abundance of this genus in human studies have been associated with intestinal inflammation and metabolic disorders (Martín et al., 2023) suggesting a relatively healthy gut in the LBF group. In addition, the increased abundance of *Treponema* is directly related to its fiber degraded function. The genus degrades complex polysaccharides in roughage to produce propionic acid via xylanase (Niu et al., 2022), which inhibits the accumulation of hepatic lipid synthesis precursors such as acetyl-CoA. *Treponema*, which is usually found in low abundance in monogastric animals, showed ruminant characteristics in TC pigs adapted to high fiber diets, which may be a result of the long-term adaptation of TC pigs to the high fiber roughage feeding pattern in the tropics the high abundance of *Treponema* not only evolved a unique metabolic strategy, but also provided a new research direction for analyzing roughage tolerance traits in local pig breeds. Enrichment of *Desulfovibrio* and *Succinivibrio* synergistically drove fat deposition in TC pigs of the HBF group. Elevated abundance of *Desulfovibrio*, although correlated with butyric acid synthesis, led to accumulation of H_2S due to its sulfate reducing property, disrupted intestinal barrier function and induced systemic inflammation, and inhibited adipose tissue β-oxidation capacity. Meanwhile, *Succinivibrio* enrichment increases the supply of hepatic lipid synthesis precursors through succinate activation of the intestinal gluconeogenesis pathway, providing a metabolic basis for fat deposition. For the further applications. This research can directly inform the creation of targeted synbiotic (combining probiotics and prebiotics) formulations. By supplementing with beneficial microbes (e.g., those that are depleted in high-backfat pigs) and the specific fibers that promote their growth, we can steer the gut microbiome towards a profile associated with leaner phenotypes. On the other hand, the key microbial taxa and liver genes identified can serve as a panel of biomarkers. Moreover, this work provides a concrete map of the gut-liver axis in the context of porcine adiposity. The correlations between specific gut bacteria and hepatic metabolic pathways (e.g., fatty acid β-oxidation, lipogenesis) offer mechanistic hypotheses.

5. Conclusions

The study revealed transcriptional networks and microbial signatures associated with fat deposition for the first time in Tunchang pigs. Key regulators included (1) *PLIN2*, *CEL*, *CYP7A1*, *AMY2* and *SLC34A2*; (2) *Desulfovibrio*, *Succinivibrio*, *Faecalibacterium*, and *Treponema* genera. This finding provides targets for regulating the fat deposition characteristics of local pig breed, which is conducive to improve the economic efficiency.

Supplementary material

The supplementary material of this article can be found online at: https://www.rbz.org.br/wp-content/uploads/articles_xml/1806-9290-rbz-55-e20250061/1806-9290-rbz-55-e20250061-suppl01.pdf

Data availability

The data presented in this study are available on request from the corresponding author.

Author contributions

Conceptualization: Huang, G. and Wang, Z. **Data curation:** Huang, G. **Formal analysis:** Zhang, Y. and He, J. **Funding acquisition:** Wang, Z. **Methodology:** Zhang, Y. and He, J. **Resources:** Wang, Z. **Software:** Zhang, Y.; He, J. and Chen, K. **Supervision:** Chen, K. **Visualization:** Peng, C. **Writing – original draft:** Huang, G. **Writing – review & editing:** Huang, G.

Conflict of interest

The authors declare no conflict of interest.

Acknowledgments

The authors acknowledge Zhejiang University for providing the necessary facilities for experimentation and data analysis.

Financial support

The research was funded by the Sanya Science and Technology Star Special Project (2024KJFX025) and Hainan Province Science and Technology Special Fund (ZDYF2022XDNY238).

References

Albuquerque, A.; Óvilo, C.; Núñez, Y.; Benítez, R.; López-Garcia, A.; García, F.; Félix, M. R.; Laranjo, M.; Charneca, R. and Martins, J. M. 2020. Comparative transcriptomic analysis of subcutaneous adipose tissue from local pig breeds. Genes 11:422. https://doi.org/10.3390/genes11040422

Aron-Wisnewsky, J.; Warmbrunn, M. V.; Nieuwdorp, M. and Clément, K. 2021. Metabolism and metabolic disorders and the microbiome: The intestinal microbiota associated with obesity, lipid metabolism, and metabolic health—pathophysiology and therapeutic strategies. Gastroenterology 160:573-599. https://doi.org/10.1053/j.gastro.2020.10.057

Chambers, K. F.; Day, P. E.; Aboufarrag, H. T. and Kroon, P. A. 2019. Polyphenol effects on cholesterol metabolism via bile acid biosynthesis, CYP7A1: A review. Nutrients 11:2588. https://doi.org/10.3390/nu11112588

Chen, Q.; Zhang, W.; Cai, J.; Ni, Y.; Xiao, L. and Zhang, J. 2022. Transcriptome analysis in comparing carcass and meat quality traits of Jiaxing Black pig and Duroc × Duroc × Berkshire × Jiaxing Black pig crosses. Gene 808:145978. https://doi.org/10.1016/j.gene.2021.145978

Deng, L.; Li, W.; Liu, W.; Liu, Y.; Xie, B.; Groenen, M. A. M.; Madsen, O.; Yang, X. and Tang, Z. 2023. Integrative metabolomic and transcriptomic analysis reveals difference in glucose and lipid metabolism in the longissimus muscle of Luchuan and Duroc pigs. Frontiers in Genetics 14:1128033. https://doi.org/10.3389/fgene.2023.1128033

El Jellas, K.; Dušátková, P.; Haldorsen, I. S.; Molnes, J.; Tjora, E.; Johansson, B. B.; Fjeld, K.; Johansson, S.; Průhová, Š.; Groop, L.; Löhr, J. M.; Njølstad, P. R. and Molven, A. 2022. Two new mutations in the *CEL* gene causing diabetes and hereditary pancreatitis: How to correctly identify MODY8 cases. The Journal of Clinical Endocrinology & Metabolism 107:e1455-e1466. https://doi.org/10.1210/clinem/dgab864

Fusco, W.; Lorenzo, M. B.; Cintoni, M.; Porcari, S.; Rinninella, E.; Kaitsas, F.; Lener, E.; Mele, M. C.; Gasbarrini, A.; Collado, M. C.; Cammarota, G. and Ianiro, G. 2023. Short-chain fatty-acid-producing bacteria: Key components of the human gut microbiota. Nutrients 15:2211. https://doi.org/10.3390/nu15092211

Han, X.; Guo, J.; You, Y.; Yin, M.; Ren, C.; Zhan, J. and Huang, W. 2018. A fast and accurate way to determine short-chain fatty acids in mouse feces based on GC-MS. Journal of Chromatography B 1099:73-82. https://doi.org/10.1016/j.jchromb.2018.09.013

Hausman, G. J.; Basu, U.; Du, M.; Fernyhough-Culver, M. and Dodson, M. V. 2014. Intermuscular and intramuscular adipose tissues: Bad vs. good adipose tissues. Adipocyte 3:242-255. https://doi.org/10.4161/adip.28546

He, J.; Zhang, Y.; Li, H.; Xie, Y.; Huang, G.; Peng, C.; Zhao, P. and Wang, Z. 2023. Hybridization alters the gut microbial and metabolic profile concurrent with modifying intestinal functions in Tunchang pigs. Frontiers in Microbiology 14:1159653. https://doi.org/10.3389/fmicb.2023.1159653

Houde, A. A.; Méthot, S.; Murphy, B. D.; Bordignon, V. and Palin, M. F. 2010. Relationships between backfat thickness and reproductive efficiency of sows: A two-year trial involving two commercial herds fixing backfat thickness at breeding. Canadian Journal of Animal Science 90:429-436. https://doi.org/10.4141/CJAS09115

Hui, D. Y. and Howles, P. N. 2002. Carboxyl ester lipase: Structure-function relationship and physiological role in lipoprotein metabolism and atherosclerosis. Journal of Lipid Research 43:2017-2030. https://doi.org/10.1194/jlr.R200013-JLR200

Kersten, S. 2014. Integrated physiology and systems biology of PPARα. Molecular Metabolism 3:354-371. https://doi.org/10.1016/j.molmet.2014.02.002

Li, X.; Lu, L.; Tong, X.; Li, R.; Jin, E.; Ren, M.; Gao, Y.; Gu, Y. and Li, S. 2023. Transcriptomic profiling of meat quality traits of skeletal muscles of the Chinese indigenous Huai pig and Duroc pig. Genes 14:1548. https://doi.org/10.3390/genes14081548

Liu, S. Q.; Xu, Y. J.; Chen, Z. T.; Li, H.; Zhang, Z.; Wang, Q. S. and Pan, Y. C. 2024. Genome-wide detection of runs of homozygosity and heterozygosity in Tunchang pigs. Animal 18:101236. https://doi.org/10.1016/j.animal.2024.101236

Lyu, W.; Xiang, Y.; Wang, X.; Li, J.; Yang, C.; Yang, H. and Xiao, Y. 2022. Differentially expressed hepatic genes revealed by transcriptomics in pigs with different liver lipid contents. Oxidative Medicine and Cellular Longevity 2022:2315575. https://doi.org/10.1155/2022/2315575

Ma, L.; Tao, S.; Song, T.; Lyu, W.; Li, Y.; Wang, W.; Shen, Q.; Ni, Y.; Zhu, J.; Zhao, J.; Yang, H. and Xiao, Y. 2024. *Clostridium butyricum* and carbohydrate-active enzymes contribute to the reduced fat deposition in pigs. iMeta 3:e160. https://doi.org/10.1002/imt2.160

Martín, R.; Rios-Covian, D.; Huillet, E.; Auger, S.; Khazaal, S.; Bermúdez-Humarán, L. G.; Sokol, H.; Chatel, J. M. and Langella, P. 2023. *Faecalibacterium*: A bacterial genus with promising human health applications. FEMS Microbiology Reviews 47:fuad039. https://doi.org/10.1093/femsre/fuad039

Niu, Q.; Pu, G.; Fan, L.; Gao, C.; Lan, T.; Liu, C.; Du, T.; Kim, S. W.; Niu, P.; Zhang, Z.; Li, P. and Huang, R. 2022. Identification of gut microbiota affecting fiber digestibility in pigs. Current Issues in Molecular Biology 44:4557-4569. https://doi.org/10.3390/cimb44100312

Pan, H.; Huang, T.; Yu, L.; Wang, P.; Su, S.; Wu, T.; Bai, Y.; Teng, Y.; Wei, Y.; Zhou, L. and Li, Y. 2022. Transcriptome analysis of the adipose tissue of Luchuan and Duroc pigs. Animals 12:2258. https://doi.org/10.3390/ani12172258

Poklukar, K.; Čandek-Potokar, M.; Batorek Lukač, N.; Tomažin, U. and Škrlep, M. 2020. Lipid deposition and metabolism in local and modern pig breeds: A review. Animals 10:424. https://doi.org/10.3390/ani10030424

Ponziani, F. R.; Pecere, S.; Gasbarrini, A. and Ojetti, V. 2015. Physiology and pathophysiology of liver lipid metabolism. Expert Review of Gastroenterology & Hepatology 9:1055-1067. https://doi.org/10.1586/17474124.2015.1056156

Portincasa, P.; Bonfrate, L.; Vacca, M.; De Angelis, M.; Farella, I.; Lanza, E.; Khalil, M.; Wang, D. Q.-H.; Sperandio, M. and Di Ciaula, A. 2022. Gut microbiota and short-chain fatty acids: Implications in glucose homeostasis. International Journal of Molecular Sciences 23:1105. https://doi.org/10.3390/ijms23031105

Qi, Y.; Jiang, C.; Cheng, J.; Krausz, K. W.; Li, T.; Ferrell, J. M.; Gonzalez, F. J. and Chiang, J. Y. L. 2015. Bile acid signaling in lipid metabolism: Metabolomic and lipidomic analysis of lipid and bile acid markers linked to anti-obesity and anti-diabetes in mice. Biochimica et Biophysica Acta – Molecular and Cell Biology of Lipids 1851:19-29. https://doi.org/10.1016/j.bbalip.2014.04.008

Qiu, Y.; Yang, X.; Ma, X.; Xiong, Y.; Tian, Z.; Fan, Q.; Wang, L. and Jiang, Z. 2017. CIDE gene expression in adipose tissue, liver, and skeletal muscle from obese and lean pigs. Journal of Zhejiang University-Science B 18:492-500. https://doi.org/10.1631/jzus.B1600294

Reiter, S. S.; Halsey, C. H. C.; Stronach, B. M.; Bartosh, J. L.; Owsley, W. F. and Bergen, W. G. 2007. Lipid-metabolism-related gene expression profiling in liver, skeletal muscle and adipose tissue in crossbred Duroc and Pietrain pigs. Comparative Biochemistry and Physiology Part D: Genomics and Proteomics 2:200-206. https://doi.org/10.1016/j.cbd.2007.04.008

Schoeler, M. and Caesar, R. 2019. Dietary lipids, gut microbiota and lipid metabolism. Reviews in Endocrine and Metabolic Disorders 20:461-472. https://doi.org/10.1007/s11154-019-09512-0

Sztalryd, C. and Brasaemle, D. L. 2017. The perilipin family of lipid droplet proteins: Gatekeepers of intracellular lipolysis. Biochimica et Biophysica Acta – Molecular and Cell Biology of Lipids 1862:1221-1232. https://doi.org/10.1016/j.bbalip.2017.07.009

Tan, Z.; Li, J.; He, Y.; Wang, F. and Xiao, Q. 2024. Characteristics of gut microbiota and metabolomics of Hainan Tunchang pigs at various growth stages. Gene 900:148161. https://doi.org/10.1016/j.gene.2024.148161

Thiengpimol, P.; Koonawootrittriron, S. and Suwanasopee, T. 2022. Genetic and phenotypic correlations between backfat thickness and weight at 28 weeks of age, and reproductive performance in primiparous Landrace sows raised under tropical conditions. Tropical Animal Health and Production 54:43. https://doi.org/10.1007/s11250-022-03047-4

Tsai, T.-H.; Chen, E.; Li, L.; Saha, P.; Lee, H.-J.; Huang, L.-S.; Shelness, G. S.; Chan, L. and Chang, B. H.-J. 2017. The constitutive lipid-droplet protein PLIN2 regulates autophagy in liver. Autophagy 13:1130-1144. https://doi.org/10.1080/15548627.2017.1319544

Wang, F.; Zha, Z.; He, Y.; Li, J.; Zhong, Z.; Xiao, Q. and Tan, Z. 2023a. Genome-wide re-sequencing data reveals the population structure and selection signatures of Tunchang pigs in China. Animals 13:1835. https://doi.org/10.3390/ani13111835

Wang, F.; Zhang, Y. B.; Jiang, Q.; Yin, Y. L.; Tan, B. E. and Chen, J. S. 2023b. Analysis of transcriptome differences between subcutaneous and intramuscular adipose tissue of Ningxiang pigs. Hereditas 45:1147-1157.

Wen, S.; He, L.; Zhong, Z.; Zhao, R.; Weng, S.; Mi, H. and Liu, F. 2021. Stigmasterol restores the balance of Treg/Th17 cells by activating the butyrate-PPARγ axis in colitis. Frontiers in Immunology 12:741934. https://doi.org/10.3389/fimmu.2021.741934

Xiao, Y.; Kong, F.; Xiang, Y.; Zhou, W.; Wang, J.; Yang, H.; Zhang, G. and Zhao, J. 2018. Comparative biogeography of the gut microbiome between Jinhua and Landrace pigs. Scientific Reports 8:5985. https://doi.org/10.1038/s41598-018-24289-z

Xing, K.; Wang, K.; Ao, H.; Chen, S.; Tan, Z.; Wang, Y.; Xitong, Z.; Yang, T.; Zhang, F.; Liu, Y.; Ni, H.; Sheng, X.; Qi, X.; Wang, X.; Guo, Y. and Wang, C. 2019. Comparative adipose transcriptome analysis digs out genes related to fat deposition in two pig breeds. Scientific Reports 9:12925. https://doi.org/10.1038/s41598-019-49548-5

Yan, S.; Zhu, C.; Yu, T.; Huang, W.; Huang, J.; Kong, Q.; Shi, J.; Chen, Z.; Liu, Q.; Wang, S.; Jiang, Z. and Chen, Z. 2017. Studying the differences of bacterial metabolome and microbiome in the colon between Landrace and Meihua piglets. Frontiers in Microbiology 8:1812. https://doi.org/10.3389/fmicb.2017.01812

Yang, H.; Xiang, Y.; Robinson, K.; Wang, J.; Zhang, G.; Zhao, J. and Xiao, Y. 2018. Gut microbiota is a major contributor to adiposity in pigs. Frontiers in Microbiology 9:3045. https://doi.org/10.3389/fmicb.2018.03045

Zhang, P.; Li, Q.; Wu, Y.; Zhang, Y.; Zhang, B. and Zhang, H. 2022. Identification of candidate genes that specifically regulate subcutaneous and intramuscular fat deposition using transcriptomic and proteomic profiles in Dingyuan pigs. Scientific Reports 12:2844. https://doi.org/10.1038/s41598-022-06868-3

Zhong, Z.; Wang, Z.; Xie, X.; Tian, S.; Wang, F.; Wang, Q.; Ni, S.; Pan, Y. and Xiao, Q. 2023. Evaluation of the genetic diversity, population structure and selection signatures of three native Chinese pig populations. Animals 13:2010. https://doi.org/10.3390/ani13122010